Supplementary Notes

These notes are intended to elaborate on the original text and to clarify various points. I have included these comments as supplemental text so as not to change the original book pagination. Each note is referenced in the text, and here to the text page to which it applies. Typographical errors have been corrected in the text.

1. page 109, discussion of the Petzold data: As I said, Petzold's volume scattering function data are "The most carefully made and widely cited ...." However, I did not say they were perfect. Although his data are undoubtedly adequate for most applications – in particular, those for which the small-angle behavior of $\beta(\psi)$ is unimportant – his values may have serious errors at scattering angles less than a few degrees. Petzold himself states (1972, page 3): "Even though care was taken to reduce the instrument's own internal scattering, it is still significant relative to the small angle forward scattering of clear water, ..." Moreover, there were almost certainly significant diffraction effects arising from the small apertures used to form the beam: his instrument could not distinguish between a small change in light direction caused by diffraction within the instrument and an equal change in direction caused by scattering within the water. (His small-angle instrument measured scattering at nominal angles of $\psi = 0.172$, 0.344, and 0.688 degrees.) I won't speculate on how big these errors might be, but I do feel that there is need for further very careful measurements of small-angle scattering. Note also that Petzold could not make measurements at values of ψ greater than 170 degrees; the values shown in Table 3.10 for 175 and 180 degrees were obtained by extrapolation.

2. page 138, first equation: If the surrounding medium absorbs, this equation uses complex division, i.e., $m_r = (n_s - ik_s)/(n_m - ik_m)$. But the surrounding medium is usually assumed to be nonabsorbing, in which case $k_m = 0$ and the equation is correct as written.

3. page 148, Section 4.1: I now realize that I *use* and discuss the interaction principle, but that I never actually *state* the principle. I omitted an explicit statement of the principle because, as Preisendorfer (1965, p. 112) states, it is

"necessarily abstract" and I was trying to spare the reader the mathematical pain associated with the principle [see *H.O.* vol II, page 205, for a mathematically rigorous statement of the principle]. However, I should have given a qualitative (even if imprecise) version of the principle, so here it is (with the key concepts italicized):

> Consider an *arbitrary region of space* (which may be a point, line, surface, or volume) in which *the laws of geometrical optics hold.* An *arbitrary incident radiance* (or irradiance, or intensity, or any other radiometric quantity) falls onto the region of space, which emits a *response radiance* (or response irradiance, etc). Then the interaction principle states: *there exists a unique set of linear (interaction) operators that connects the response radiance with the incident radiance.*

The profound significance of the interaction principle is this: *It guarantees us that if we want to find the response radiance induced by a given incident radiance falling onto a given region of space* (e.g. a particular region of a water body), *we can expend our efforts in finding the linear interaction operators for the spatial region of interest.* Once these operators are known, we then simply use them to "operate" on the given incident radiance to get the desired response radiance.

I missed a golden opportunity here to give the reader a "heads up" on how the interaction principle will be used at several places in the book, so let me do it now:

> Much of Chapter 4 is devoted to showing how to numerically estimate the four interaction operators (the radiance transfer functions) that connect incident and response radiances for a wind-blown air-water surface. Here, the arbitrary region of space mentioned above is a two-dimensional surface, and the "operation" is the integrations seen in Eqs. (4.3) and (4.4).
>
> Another example of the interaction principle is seen in the path function for elastic scattering, Eq. (5.5). Here the interaction operator is the volume scattering function, which is assumed to be given, and the region of space is the point at which the scattering occurs. Although we derive Eq. (5.5) from physically based arguments, we could write it down immediately after invoking the interaction principle (but recall my comments in the third paragraph of page 236).

In Chapter 7 we show how interaction operators can give the response irradiances for a finitely thick layer of water; see, for example, Eqs. (7.47) and (7.48) on page 361. Here the region of space is the (infinite) volume (layer) of water between two different depths, the interaction operators are certain reflectances and transmittances for the layer of water, and the operations are simple multiplications. We develop a set of differential equations that are easily solved for the desired operators (the Riccati equations of Section 7.8).

In Chapter 8, we show how interaction operators can give us certain Fourier amplitudes of the radiance distribution (from which we can compute the desired radiance). Once again, the region of space is the layer of water between two depths. The interaction operators are matrices composed of certain reflectance and transmittance functions for the layer of water, and matrix multiplication is the operation that converts incident radiance amplitudes into response radiance amplitudes. The operators are again obtained from Riccati differential equations. See Eqs. (8.70) and (8.71) for the appropriate form of the interaction principle, and see Eqs. (8.74)-(8.85) for the Riccati equations that give us the needed operators.

4. page 157, Eq. (4.14b): Strictly speaking, this equation should use the complex index of refraction, with an absolute value squared. But for water at near UV to near IR wavelengths, the difference is negligible if only the real part of the index of refraction is used.

5. page 168, discussion: I should had added more discussion here. The wave-slope wind-speed Eqs. (4.32) are often called (as I did here) the Cox-Munk *capillary* wave slope equations. This is permissible, because the equations do give the slopes of capillary waves fairly well. However, it should be emphasized that these equations also represent the slopes of a gravity-capillary wave surface. Recall that Duntley measured the slopes of capillary waves, and Cox and Munk deduced (indirectly, from an airplane) the slope statistics of a gravity-capillary wave surface. The fact that these two quite different experiments gave nearly the same results rests on the fact that most of the variance in the *slope* of the sea surface is due to the shortest wavelength (capillary) waves. Most of the variance in the *amplitude* of the surface waves is due to the longest (gravity) waves. For optics, it is the slope of the surface that is most important because the slope determines the angles entering the

Fresnel reflectance equations for an incident ray. The amplitude of the waves determines the amount of wave "shadowing" at low solar elevations and influences multiple scattering between gravity waves, but these effects are secondary except for near-grazing lines of sight and near-horizon sun positions. Thus Eqs. (4.32) can be used to model a gravity-capillary sea surface with reasonable accuracy for many oceanographic purposes. This is what is done in Hydrolight, as discussed in the next note.

6. page 228, Eq. (4.79): The four equations down to and including the k_{uv} = ... equation are completely general. The equations starting with $F(\sigma_{uv}, \phi_{uv})$ = ... define the SWOP spectrum. The SWOP spectrum is now quite out of date. The latest, greatest gravity-capillary wave spectrum I've run across is Elfouhaily, T., B. Chapron, K. Katsaros, and D. Vandemark, 1997. A unified directional spectrum for long and short wind-driven waves, *J. Geophys Res.* 102(C7), 15781-15796 (1997); but note that this paper has a typo: its Eq. (41) should read $F_m = L_{pm}\, J_p \exp\{...\}$. This paper is called ECKV below.

Hydrolight uses Monte Carlo ray tracing of millions of rays (or photon packets) through tens of thousands of randomly generated sea surface realizations to compute the radiance reflectance and transmittance functions that describe the optical effects of the sea surface (see section 4.7). When doing Monte Carlo simulations of rays interacting with the sea surface, it is the slope of the surface at the point where a ray intersects it that determines the directions of the reflected and transmitted rays, and the associated Fresnel reflectance and transmittance. Thus if the slope statistics are correct, which they are in Hydrolight, the optical effects of the surface will be accurately modeled in most situations. The exception may occur if the sun or viewing direction is near the horizon. Then effects such as wave shadowing by large gravity waves may become important (see Fig. 4.32). Modeling wave shadowing by gravity waves requires that the sea surface elevation statistics also be correct and that the larger gravity waves be properly modeled, which is not the case in Hydrolight (or in any other optical oceanography radiative transfer model of which I'm aware). Note, however, that Hydrolight does include multiple scattering between wave facets.

ECKV give a comprehensive directional wave spectrum valid for the full range of gravity and capillary waves. In their notation, the mean square slope (mss) of the sea surface is given by (ECKV Eq. A6)

$$mss = \int_0^\infty S(k)\, k^2\, dk\,, \qquad \text{(SN.1)}$$

where $S(k)$ is the omnidirectional (1D) elevation spectrum and k is the wave number. $S(k)k^2$ is then the omnidirectional slope spectrum. The Cox-Munk mss is given by (ECKV Eq. 26)

$$mss = 10^{-3}(3 + 5.12\,U_{10}) \pm 0.004\,, \qquad \text{(SN.2)}$$

where U_{10} is the wind speed in meters per second at 10 m elevation. Equation (SN.1) can be numerically integrated for a given wind speed, using the elevation spectrum given in ECKV. When this is done for U_{10} = 6 m s^{-1}, for example, Eq. (SN.1) gives *mss* = 0.036. The corresponding Cox-Munk value obtained from Eq. (SN.2) is *mss* = 0.034 ± 0.004. This good agreement between the Cox-Munk *mss* and *mss* computed from the full gravity-capillary wave spectrum shows that Cox-Munk (hence Hydrolight) does indeed properly describe the slope statistics of a fully developed wind-blown surface.

However, there are differences in how Hydrolight models the sea surface compared to a surface generated by resolving all wavelengths of the ECKV spectrum. Hydrolight uses the Cox-Munk wave slope statistics to model a hexagonal patch of sea surface as a number of triangular wave facets, as described in §4.3. The vertex elevations of these triangular facets are spatially uncorrelated, because the Cox-Munk equations do not contain spatial correlation information. Figure SN.1(a) shows a patch of sea surface approximately 0.35 m on a side, covered with numerous small wave facets as generated by Hydrolight for U_{10} = 6 m s^{-1}. The resulting sea surface has a crinkly and somewhat unphysical appearance, even though the slopes of the triangular facets are statistically correct. [In Fig. SN.1, there are n_{hex} = 50 "rings" of triangular wave facets around the center of the hexagonal patch of sea surface, compared to n_{hex} = 2 in Fig 4.2. The 7,651 points where the surface elevation is computed are shown by the dots making up the hexagon below the surface elevation plot.]

The ECKV directional (2D) spectrum can be used to generate sea surface realizations that do have spatial correlation from one triangle vertex to the next, as described in §4.9 (after replacing the outdated SWOP spectrum with ECKV). Figure SN.1(b) shows an example realization of the resulting surface for the same hexagonal patch of water as seen in Fig. SN.1(a). The surface now resolves the smaller gravity waves and capillary waves. The surface elevation is spatially correlated from each point to the neighboring points, and the surface appears more realistic than that of Fig. SN.1(a). If we back off from the surface, we see the effects of the largest gravity waves. Figure SN.1(c) shows a patch of sea surface approximately 70 m on a side.

This figure resolves only the largest gravity waves of the ECKV directional spectrum. Figure SN.1(b) can be thought of as a small patch of sea surface riding on the Fig. SN.1(c) surface at the middle of the large hexagonal surface patch.

Computing the variance of the alongwind slope, mss_x, for the row of surface elevation points at $y = 0$ in Fig. SN.1(a) gives $mss_x = 0.01866$. This compares well with the theoretical value of $mss_x = 0.01896$ (Eq. 4.32). This (and many other similar checks) shows that Hydrolight is simulating sea surfaces consistent with the Cox-Munk slope statistics.

The classic Cox-Munk slope statistics as expressed by Eq. (SN.2) agree with the sophisticated ECKV spectrum predictions of Eq. (SN.1), which supports the use of the Cox-Munk equations without modification. Shifrin (Shifrin, K. S., 2001. An algorithm for determining the radiance reflected from the rough sea surface using MODIS-N satellite radiometer data, *IEEE Trans. Geosci. Rem. Sens*., **39**(3), 677-681.), however, has synthesized recent work on slope statistics and concluded that the slope variance given by Cox and Munk for a given wind speed U_{10} is too small by a factor of 1.45 for a neutrally stabile marine atmospheric boundary layer. Shifrin's conclusions imply (his Eq. 21) that U_{10} in Eq. (SN.2) should be replaced by $1.45U_{10} + 0.27$. To make a Hydrolight run consistent with Shifrin's recommendation, a classic 6 m s^{-1} wind speed, for example, should be entered into Hydrolight as a 9 m s^{-1} wind speed (= 1.45 × 6 + 0.27). Shifrin also shows how to incorporate atmospheric stability effects on sea surface roughness into the Cox-Munk equations.

(a)

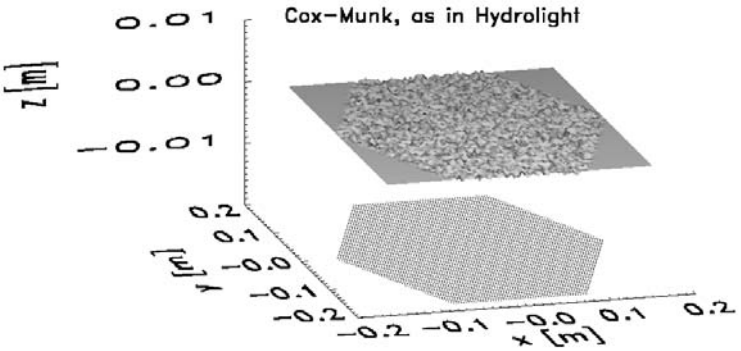

(b)

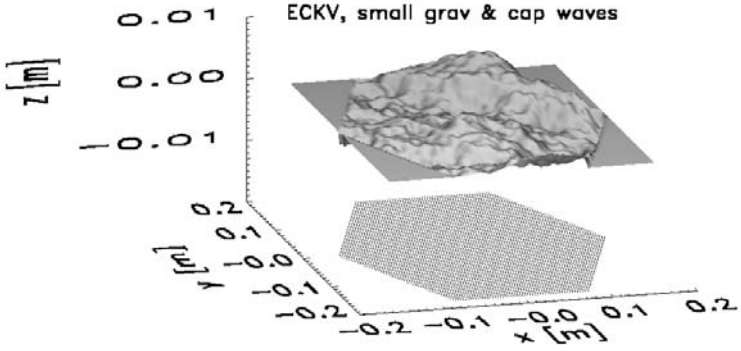

(c)

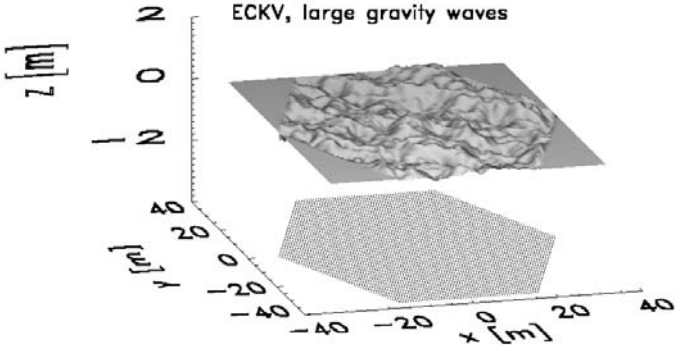

Fig. SN.1. Realizations of a random sea surface for U_{10} = 6 m s^{-1} and n_{hex} = 50. x is the alongwind direction, y is crosswind, and z is surface elevation.

The way Hydrolight models wind-blown sea surfaces can be summarized as follows:

- Hydrolight properly simulates the slope statistics of a fully developed gravity-capillary sea surface for a given wind speed. It therefore properly simulates radiative transfer across wind-blown surfaces for solar zenith angles and viewing directions that are not very near the horizon.

- Hydrolight does include multiple scattering between the triangular wave facets used to generate surface realizations.

- Hydrolight does not simulate the elevation statistics of a wind-blown surface. Therefore, it does not account for effects such as wave shadowing of the "back" sides of large gravity waves when the sun is near the horizon. Such effects may be important in some situations (e.g., near sun rise or sun set), but quantitative studies have not been made.

- Hydrolight does not simulate the spatial correlation statistics of wind-blown sea surfaces, so any effects that depend on spatial correlations (e.g., of correlated capillary wave trains riding on the faces of larger gravity waves) are not accounted for. Such effects are unlikely to be important at visible wavelengths for most (but not all) applications.

- Hydrolight does not include effects of atmospheric stability on surface roughness, but such effects can be incorporated into a Hydrolight run by entering a modified wind speed.

- Hydrolight does not include effects of foam generated by whitecaps at high wind speeds.

One question remains: why don't I just start using surfaces generated by the ECKV directional spectrum and properly model all surface statistics. The answer is simply insufficient computer power. Generating Fig. SN.1(b) or SN.1(c) takes ~2,500 times longer than generating Fig. SN.1(a). Moreover, one should in principle resolve all relevant wave scales from the largest gravity waves [as in Fig SN.1(c)] to the smallest capillary waves [as in Fig. SN.1(b)]; doing so would increase the computer time by another enormous factor. Given that I need to generate tens of thousands of surfaces to build up good statistical estimates of the surface radiative transfer properties, such computations are, for the moment, beyond reach (although they would be great fun to do!).

7. page 237 and following pages: I should have commented that terms like "transpectral scattering," "inelastic absorption," and "true absorption" are not standard terminology in physics or chemistry. These terms are seen (as far as I know) only in the oceanic optics literature, where they can be traced back to page 65 of Preisendorfer's 1965 book. A spectroscopist would use "inelastic scattering" not "transpectral scattering", "absorption" rather than "true absorption," and "inelastic scattering" in place of "inelastic absorption." It was a mistake to use Preisendorfer's nonstandard terminology, so I recommend sticking with what is standard in the literature.

8. page 245, Eq. (5.11): I should have noted that there is no standard term in the literature for my quantity b^{I}, although Gordon (1979) calls a corresponding quantity (Φ in his Eq. 2) "the coefficient of fluorescence." In Gordon, et al, (1993), *Appl. Optics* 32, page 1617 he calls b^{I} the "total scattering coefficient for fluorescence."

9. page 265 and following: My extensive discussion of the two-flow equations has been criticized because it makes them appear more important than they really are. I agree with this, but I wanted to treat them in detail to show exactly what goes into them and to make clear what problems are associated with them. As I emphasized on page 270, the two-flow equations are useless for predictive purposes and, as I discussed on pages 480 and 481, they are of limited use for inverse modeling. Our exploitation of the two-flow equations, e.g. in Section 5.12 and in Chapter 7, has milked them for all they are worth. I should have emphasized that *it is past time to lay the two-flow equations to rest, considering how easy it is to solve the RTE with a modern computer and get the full radiance distribution, thereby avoiding all of the problems inherent in the two-flow equations*.

10. page 321, line 5 from the bottom: Note that there is no cosine factor (as in Eqs. 1.23 and 1.24) in the computation of plane irradiance when you are counting individual photons in Monte Carlo simulations. The cosine factor appears in radiance equations, e.g., Eqs. (1.23) and (1.24) to account for the decreased area of the detector as seen from a given direction. The decreased area of the detector is automatically accounted for in Monte Carlo simulations because photons are less likely to hit the detector when coming from off-axis directions.

11. page 341, Chapter 7: Chapter 7 has been criticized as being "really hard," or something to that effect but more emphatic and poetic. I wholeheartedly agree – it took me years to learn this stuff.

Remember, as I said on page 343, one of the goals of this book is to give the most important results from Preisendorfer's *Hydrologic Optics*, and that's what I tried to do in this chapter. I thought that the use of the two-flow equations (rather than starting with the RTE) was a clever way to discuss fundamental and transport solutions (and other such things) with a *minimum* of math, as well as setting the stage for solving the RTE in Chapter 8. I know that the notation, with all of the $\mathbf{m}_{\pm\pm}$ and $\mathbf{M}_{\pm\pm}$ and so on, is confusing, but that is what is standard in the literature.

In Section 7.2 I tried to give an overview of what was coming in the chapter, but I failed to explain this at the beginning; my apologies. I should have emphasized that the ultimate goal of our development was to obtain the Riccati equations of Section 7.8, and I should have elaborated on the extreme importance of those equations: *it is the Riccati equations that give us the operators whose existence is guaranteed by the interaction principle*. In the present case, the linear interaction operators are the standard reflectances and transmittances, and the operation that converts incident irradiances into response irradiances is simple multiplication, as seen in Eqs. (7.47) and (7.48). Once again, note that we have transformed a problem in which we solve directly for the irradiances (by explicitly integrating the two-flow equations) into a problem in which we solve for certain "operators" (the reflectances and transmittances, as well as the source-induced irradiances, by integrating the Riccati equations). See Supplementary Note 3.

12. page 457, second paragraph: The reference to Højerslev and Zaneveld (1979) should be 1977. An additional comment is warranted here. I stated on page 262 that "Preisendorfer (1959 ...) proves the general result that ... [an asymptotic radiance distribution exits under certain reasonable conditions]." Strictly speaking, Preisendorfer (1959) showed that *if* the diffuse attenuation coefficient for scalar irradiance, K_o, approaches a constant at great depths in homogeneous water (i.e., if the scalar irradiance decays exactly exponentially with depth, and with some other reasonable assumptions), *then* an asymptotic radiance distribution exists. He then invoked observational evidence to justify the assumption of a constant K_o at great depths in homogeneous water. Højerslev and Zaneveld (1977) gave a proof without resorting to the assumption about K_o, and that is why I credited them with "the first rigorous

mathematical proof," i.e. a proof that does not need to invoke observational evidence. However, upon rereading these and related papers, I note that Preisendorfer also gives a proof without the offending assumption in *H.O.* vol 5, beginning on page 212, which was published in 1976. I'll now leave it to the historians squabble about who was first with a "real" proof.

13. page 476, section on the Wells radiometer: I commented that "Wells (1983) performed a decomposition of L and β similar to that seen in Eq. (10.2) [which came from Zaneveld (1974)]." However, there is an earlier paper by Zaneveld and Pak (*J. Geophys. Res*. 77(15), 2677-2680, 1972) that both Wells and I should have referenced. The Zaneveld and Pak paper performed the decomposition seen in Eq. (10.2) and repeated in Wells (1983) and – most importantly – went on to clearly describe how one could retrieve IOP's from measurements of the moments of the radiance distribution. It thus seems fair to credit Zaneveld and Pak (1972) with the original idea, and to credit Wells (1983) with rediscovering the idea and then describing in detail how to construct an instrument to measure the radiance moments.

<< Table of Contents